NJC

Accepted Manuscript

This is an *Accepted Manuscript*, which has been through the Royal Society of Chemistry peer review process and has been accepted for publication.

Accepted Manuscripts are published online shortly after acceptance, before technical editing, formatting and proof reading. Using this free service, authors can make their results available to the community, in citable form, before we publish the edited article. We will replace this *Accepted Manuscript* with the edited and formatted *Advance Article* as soon as it is available.

You can find more information about *Accepted Manuscripts* in the Information for Authors.

Please note that technical editing may introduce minor changes to the text and/or graphics, which may alter content. The journal's standard Terms & Conditions and the Ethical guidelines still apply. In no event shall the Royal Society of Chemistry be held responsible for any errors or omissions in this *Accepted Manuscript* or any consequences arising from the use of any information it contains.

ROYAL SOCIETY OF CHEMISTRY

www.rsc.org/njc

NJC

RSCPublishing

LETTER

Multi-component luminescent lanthanide hybrids of both functionalized IRMOF-3 and SBA-15

Cite this: DOI: 10.1039/c3nj00000x

Xiao Lian, and Bing Yan*

Received 00thXXXXX 2013,
Accepted 00thXXXXX 2013

DOI: 10.1039/c3nj00000x

www.rsc.org/njc

Both metal organic frameworks (IRMOF-3) and SBA-15 have been used to assemble novel photofunctional multi-component lanthanide hybrid materials (Ln-SBA-15-Si-IRMOF-3, Ln = Eu, Tb, Nd, Yb), whose luminescent color can be tuned by adjusting the composition.

Lanthanide ions attract great interest for their sharp and intense emission bands, broad range of lifetimes and high color purity,[1] whose complexes exhibit efficient emission under ultraviolet excitation.[2] In order to improve the luminescent stability of lanthanide complexes, all kinds of lanthanide hybrid materials are developed to compose the respective character of inorganic and organic units, which have many potential applications in the fields of optical amplifiers and light-conversion molecular devices *etc*.[3,4] It needs to be referred that the key is to design a functional linker both coordinating and sensitizing lanthanide ions for the whole hybrid system.[5]

Furtherly, lanthanide mesoporous silica hybrids can be prepared in the presence of surfactants or other templates, which combine the luminescence properties of lanthanide complexes and the structural properties of mesoporous materials. These researches involve some kinds of typical mesoporous host such as MCM-41(48), SBA-15(16) and periodical organic mesoporous silica (POMs), *etc*.[6-8] The hybrid materials enable both inorganic and organic dopants to be incorporated with relatively high thermal stability. Among all of the mesoporous materials, SBA-15 is paid much more attractive than other mesoporous silica for its adjustable pore size (3 to 30 nm), large pore-size mesochannel, thick silica wall and high thermal stability.[9] Besides, both mesoporous SBA-15 and microporous zeolite have a large number of hydroxyls, which can be easily further functionalized to assemble hybrid materials together. Based on zeolite and SBA-15's capability of self-assembly of commonality, they can be linked together by silane coupling agent and coordinated lanthanide ion.[10] The new synthetic micro-mesoporous hybrid materials have the advantages over either microporous or mesoporous materials.[10]

Metal-organic frameworks (MOFs) are a class of crystalline systems, which are assembled with metal ions and organic ligands in appropriate conditions.[11] As a permanently microporous materials, MOFs have drawn sustained attention for their unique properties such as large specific surface area, ordered crystalline structure, and highly rule-pores. So MOFs have lots of potential applications, among which the most important application is encapsulating a variety of functional species into these peculiar host frameworks to increase or enhance their properties such as luminescence.[12,13]

Considering the versatile chemical modification, different hosts can be further assembled together. In this work, we prepare a series of lanthanide hybrid materials containing both MOFs and SBA-15 through the multi-component assembly strategy, which is named as Ln-SBA-15-Si-IRMOF-3 (Ln = Eu, Tb, Nd, Yb). The physical characterization and luminescent properties are discussed and compared in details.

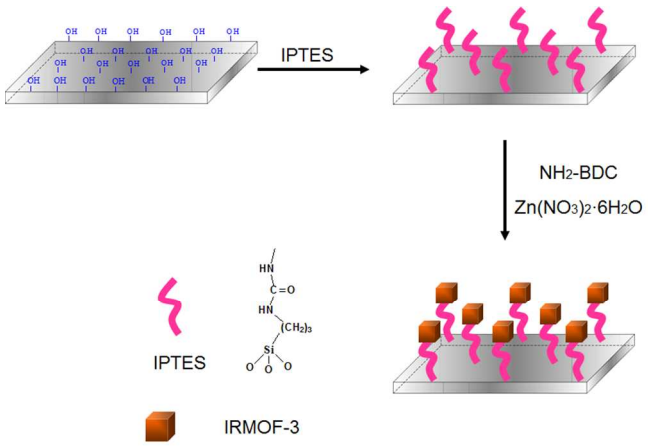

Figure 1 The selected scheme for the composition of hybrid materials Ln-SBA-15-Si-IRMOF-3 (Ln = Eu, Tb, Nd, Yb).

Figure 1 shows the scheme for the composition of the whole hybrid system, whose detailed preparation process and reaction principle are shown in the electronic supporting information (Figure S1). SBA-15 can be easily modified by the crosslinking reagent IPTES to form the Si-SBA-15 through the co-hydrolysis and co-polycondensation process between the alkoxyl groups of IPTES and hydroxyl groups of SBA-15. On the other hand, IRMOF-3 is in-situ synthesized and then is covalently grafted to Si-SBA-15 through the addition reaction between its amino group and inner ester group of Si-SBA-15. Finally, lanthanide ions (Eu^{3+}, Tb^{3+}, Nd^{3+}, Yb^{3+}) are introduced into SBA-15-Si-IRMOF-3 host through the coordination reaction.

Figure S2 shows the selected small angel X-ray diffraction patterns (SAXRD) of the prepared SBA-15 and IPTES modified Si-SBA-15, which shows the typical character of highly uniform mesoporous materials. It can be observed that a strong diffraction peak is centered at 0.8 °,corresponding to the (100) Bragg diffraction of SBA-15. There are also two obvious weak shoulder peaks locating at 1.2 and 1.6 °, respectively, which are ascribed to (110), (200) featured diffraction of SBA-15.[14] These characteristics evidence the existence of two dimension cubic pore structures and hexagonal symmetry of the space group P6mm in these three hybrids. Comparing with Figure S2 (top), the location of Bragg diffraction peaks in Figure S2 (bottom) for functionalized mesoporous silica with the introduction of IPTES don't change too much, demonstrating that the entrance of organic compounds has little influence on the three dimensional structures of the mesoporous SBA-15. Figure S3 shows the comparison IRMOF-3, SBA-15-Si-IRMOF-3 and Eu-SBA-15-Si-IRMOF-3 hybrid system. It can be seen that the XRD pattern of SBA-15-Si-IRMOF-3 and Eu-SBA-15-Si-IRMOF-3 mainly show the characteristic bands of IRMOF-3 except for the disappearance of peak at small angle of 7 °. This may be due to the modification of amino group of IRMOF-3, which affects the crystallinity of IR-MOF-3 framework.

Figure S4 gives the FT-IR spectra of Si-SBA-15 and SBA-15-Si-IRMOF-3, respectively. In the case of the SBA-15 host material, the obvious absorption bands from Si–O–Si (ν_{as}, 1081 cm^{-1}; ν_{s}, 805 cm^{-1}), Si–OH (ν_{s}, 962 cm^{-1}), Si–O (δ, 461 cm^{-1}) and H_2O (1630 cm^{-1}) are present. (Where ν_s represents symmetric stretching, ν_{as} asymmetric stretching, and δ bending) [10] Comparing with IRMOF-3-Si-SBA-15, the hybrid mesoporous materials not only exhibit the similar infrared absorption bands as the silica framework but also the peaks at 1360-1560 cm^{-1} range in SBA-15-Si-IRMOF-3, which is just originated from the –CONH– group of IRMOF-3-Si, indicating that IRMOF-3 has been grafted onto the wall of SBA-15. Figure S5 shows the FT-IR spectra of multi-component hybrids Ln-IR-SBA-15-Si-IRMOF-3 (Ln = Eu, a; Tb, b; Sm, c; Dy, d), which shows the similar features for the same SBA-15-Si-IRMOF-3 units except for different lanthanide ions in the hybrid system.

The hexagonal porous structures of selected TEM micrographs of both SBA-15-Si-IRMOF-3 and Eu-SBA-15-Si-IRMOF-3 are further confirmed by its selected (see Figure 2), which is also agreement with the result of SAXRD. As shown in the figure, both SBA-15-Si-IRMOF-3 (a,c) and Eu SBA-15-Si-IRMOF-3 (b,d) present a regular hexagonal array of uniform channels characteristic of mesoporous SBA-15 material. The distance among mesopore is estimated to be 10 nm, in good agreement with the value determined from the corresponding SAXRD data. These photos illustrate that the mesostructure of the micro-mesoporous complex materials can be substantially conserved after the coordination process.

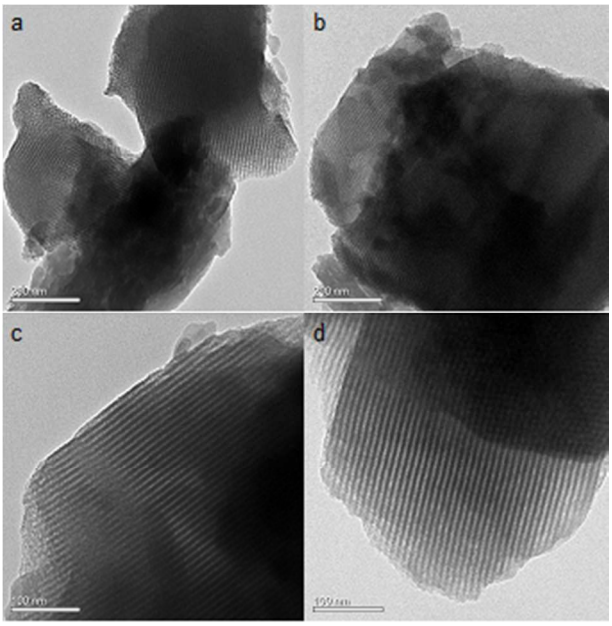

Figure 2 HRTEM images of SBA-15-Si-IRMOF-3(a,c) and Eu-SBA-15-Si-IRMOF-3 (b,d) hybrids recorded along the [100] (a,b) and [110] (c,d) zone axes.

Figure 3 shows the excitation and emission spectra of the four lanthanide hybrids with IRMOF-3 and SBA-15 units, Ln-SBA-15-Si-IRMOF-3 (Ln = Eu, Tb), all of which show the characteristic luminescence of lanthanide ions except for the different intensities of lanthanide hybrid systems. The excitation spectrum of Eu-SBA-15-Si-IRMOF-3 hybrids is obtained by monitoring the $^5D_0 \rightarrow {}^7F_2$ transition line at 613 nm, and the emission spectrum was obtained by excitation at 297 nm. A broad band ranging from 230 to 350 nm is mainly from the functionalized IRMOF-3-Si-SBA-15 host to form charge transfer state of Eu-O, whose wide excitation is favourable for the energy transfer and luminescence of Eu^{3+} in the hybrid system. Furthermore, two weak sharp excitation lines overlapped with the wide band at 393 nm and 464 nm can be observed, which correspond to f-f ($^7F_0 \rightarrow {}^5L_6$ and $^7F_0 \rightarrow {}^5D_2$) transitions of Eu^{3+} ion, respectively.[15] The corresponding emission spectrum consists of five prominent lines at 578, 590, 613, 651 and 700 nm, which are ascribed to the $^5D_0 \rightarrow {}^7F_0$, $^5D_0 \rightarrow {}^7F_1$, $^5D_0 \rightarrow {}^7F_2$, $^5D_0 \rightarrow {}^7F_3$ and $^5D_0 \rightarrow {}^7F_4$ transitions of Eu^{3+}. The hypersensitive forced electronic dipole $^5D_0 \rightarrow {}^7F_2$ transition shows the highest emission intensity. For Tb-IRMOF-3-Si-SAB-15 hybrids, its excitation spectrum obtained by monitoring the $^5D_4 \rightarrow {}^7F_5$ at 545 nm shows the narrow band ranging from 220 to 400 nm, which is ascribed to functionalizedSBA-15-Si-IRMOF-3 host. No detectable absorption lines of Tb^{3+} ions can be observed from the excitation spectra, indicating that an effective energy transfer occurs from IRMOF-3-Si-SBA-15 to Tb^{3+} ions. Under the excitation using this broad band of 320 nm, four sharp emission lines at 489, 544, 583 and 622 nm appear, which can be ascribed to the transitions of Tb^{3+}: $^5D_4 \rightarrow {}^7F_6$, $^5D_4 \rightarrow {}^7F_5$, $^5D_4 \rightarrow {}^7F_4$ and $^5D_4 \rightarrow {}^7F_3$, respectively. The emission intensity for $^5D_4 \rightarrow {}^7F_5$

transition shows the highest, which can account for the characteristic green color of Tb^{3+}.

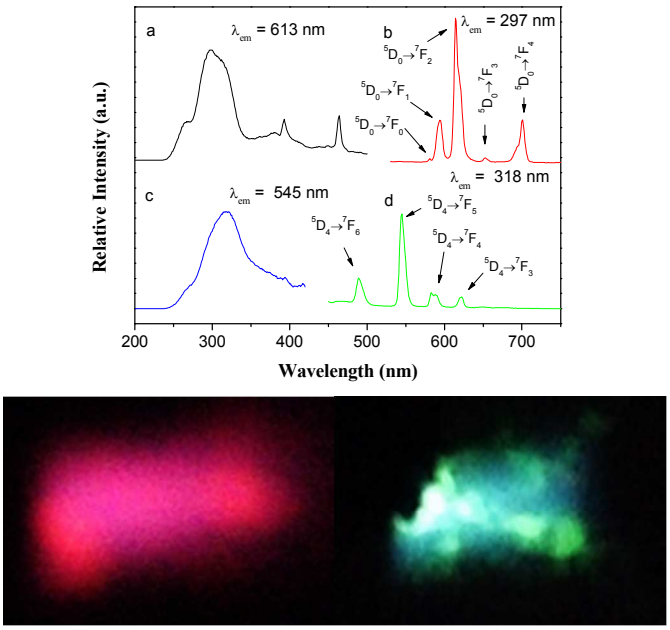

Figure 3 Luminescent excitation (a, c) and emission (b, d) spectra of the hybrids Ln-SBA-15-Si-IRMOF-3 (Ln = Eu (a, b), Tb (c, d)), the bottom is the CIE chromaticity diagram (left, Ln = Eu; right, Ln = Tb)

The luminescent quantum efficiencies of the four lanthanide hybrids are determined. Among Eu-SBA-15-Si-IRMOF-3 and Tb-SBA-15-Si-IRMOF-3 hybrids are 4.1 % and 10.1 %, respectively, corresponding to the luminescence of Eu^{3+} and Tb^{3+}. Furthermore, the CIE chromaticity diagrams of selected Eu-SBA-15-Si-IRMOF-3 and Tb-SBA-15-Si-IRMOF-3 hybrids are checked and shown in Figure S6, which are located in red (0.6041, 0.3390) and green region (0.2716, 0.4507), respectively. For Eu-SBA-15-Si-IRMOF-3 hybrids in Figure S7 (a), close white color luminescence (0.3760, 0.2410) can be integrated with suitable excitation wavelength (270 nm). For Eu/Tb-SBA-15-Si-IRMOF-3 hybrids in Figure S7 (b), the emission integration of both Eu^{3+} and Tb^{3+} appears in white region (0.3605, 0.3120).

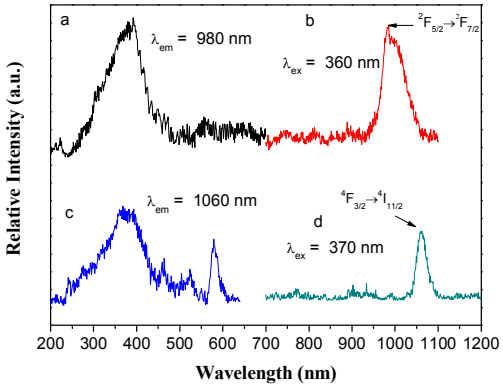

Figure 4 Luminescent excitation (a, c) and emission (b, d) spectra of the hybrids Ln-SBA-15-Si-IRMOF-3 (Ln = Yb (a, b), Nd (c, d)).

Figure 4 shows the selected emission spectra of hybrid materials Yb-SBA-15-Si-IRMOF-3 and Nd-SBA-15-Si-IRMOF-3 hybrids. Yb-SBA-15-Si-IRMOF-3 hybrids display the typical Yb^{3+} emission (950-1050 nm), with the peak around 980 nm assigned to the $^2F_{5/2} \rightarrow ^2F_{7/2}$ transition under 360 nm excitation.[16] For Nd-SBA-15-Si-IRMOF-3 hybrids, a dominant sharp emission peak at 1060 nm can be checked and is contributed by the typical luminescent transition of $^4F_{3/2} \rightarrow ^4I_{11/2}$ of Nd^{3+} under the excitation of the wavelength of 370 nm.[17] So in the hybrid systems, the near infrared luminescence for Yb^{3+} and Nd^{3+} can be obtained through the energy transfer from SBA-15-Si-IRMOF-3 unit.

In summary, we have assembled novel series of lanthanide hybrids with both functionalized IRMOF-3 and SBA-15 host through 3-isocyanatopropyltriethoxysilane (IPTES) as chemical linkage. The characteristic luminescence of Ln^{3+} in both visible and near infrared region can be obtained and even white luminescence can be integrated. The results may provide a novel strategy to assemble luminescent lanthanide hybrids, which is expected to have some potential application in practical optical fields.

Experimental

Start materials Lanthanide chlorides $LnCl_3 \cdot 6H_2O$ (Ln = Eu, Tb, Nd, Yb) were prepared by dissolving their respective oxides in concentrated hydrochloric acid with heating and stirring to promote the reaction. 3-isocyanatopropyltriethoxysilane (95 %, IPTES) was from Adamas. Triblock copolymers P123, 2-aminoterephthalic acid (99 %) were from Sigma-Aldrich. Tetraethoxysilane (TEOS, 98 %) and zinc nitrate hexahydrate ($ZnNO_3 \cdot 6H_2O$, 99 %) were from Aladdin. All the other reagents are analytical pure.

Synthesis of the isocyanate-functionalized SBA-15 mesoporous material (Si-SBA-15) The mesoporous material SBA-15 was synthesized according to the previous reported literature. P123 (1.0 g) was dissolved in deionized water (30 mL) and 12 $mol \cdot L^{-1}$ hydrochloric acid (5 mL) firstly and stirring the mixed solution until obtained a clear solution. Then added TEOS (2.3 mL, 0.011 mol) into the above solution drop by drop with stirring for 24 h at 308 K. The mixture was heated further in a polytetrafluoroethylene (PTFE)-lined steel autoclave for the hydrothermal reaction for 48 h at 373 K. The white product was washed with deionized water and ethanol after filtration and dried for 12 h at 333 K. To remove the triblock copolymers P123, the product was heating at 813 K for 5 h. For functionalization, the as-synthesized SBA-15 (0.2 g) was dispersed intetrahydrofuran (THF, 50 mL) and added 3-isocyanatopropyltriethoxysilane (IPTES, 0.2 mL, 8.1×10^{-4} mol) into the above mixture. Further, heating the mixture at reflux for 20 h under argon gas and dried the product at vacuum.

Synthesis of SBA-15-Si-IRMOF-3 The synthetic method of isoreticular metal-organic framework-3 (IRMOF-3) was described in the literature. Herein, we synthesized IRMOF-3-Si-SBA-15 via an 'in situ' process. The Si-SBA-15 (0.02 g), 2-aminoterephthalic acid (0.165 g, 9.1×10^{-4} mol) and $ZnNO_3 \cdot 6H_2O$ (0.727 g, 2.4×10^{-3} mol) were added in N, N-dimethylformamide (DMF, 50 mL), transfer the mixture into autoclave and placed in an oven at 373 K for 18 h to yield yellow cubic crystals. After centrifugation and washed with

DMF three times, the crystals was immersed in $CHCl_3$ for 3 days with fresh $CHCl_3$ replenished every 24 h.

Synthesis of lanthanide hybrid material The modified material (0.05 g) was dissolved in 3.0 mL ethanol with stirring, and then added 2.0 mL $LnCl_3$ (0.1 $mol \cdot L^{-1}$, Ln = Eu, Tb, Nd, Yb) to the solution, continuously stirring for about 12 h. After centrifugation and purification and dried at 323 K, the final material Ln-SBA-15-Si-IRMOF-3 was obtained. The relevant elemental analyses data were shown in ESI.

Notes and references

[a] *Department of Chemistry, Tongji University, Siping Road 1239, Shanghai 200092, China. E-mail: byan@tongji.edu.cn*

Electronic Supplementary Information (ESI) available: See DOI: 10.1039/b000000x/

1 (*a*) J. C. G. Bunzli and C. Piguet, *Chem. Rev.*, 2005, **34**,1048; (*b*) (*a*) J. C. G. Bunzli, *Acc. Chem. Res.*, 2006, **39**,53.

2 (*a*) P. Gawryszewska, J. Sokolnicki and J. Legendziewicz, *Coord. Chem. Rev.*, 2005, **249**,2489; (*b*) Y. Ma and Y. Wang, *Coord. Chem. Rev.*, 2010, **254**, 972; (*c*) A. D'Aleo, F. Pointillart, L. Ouahab, C. Andraud and O. Maury, *Coord. Chem. Rev.*, 2012, **256**, 1064.

3 (*a*) L. D. Carlos, R. A. S. Ferreira, V. D. Bermudez and S. J. L. Ribeiro, *Adv. Mater.*, 2009, **21**, 509; (*b*) K. Binnemans, *Chem. Rev.*,2009,**109**,4283; (*c*) B. Yan, *RSC Adv.*, 2012, **2**, 9304; (*d*) J. Feng, H. J. Zhang, *Chem. Soc. Rev.*, 2013, **42**, 387.

4 (*a*) J. Silver and R. Withnall, *Chem. Rev.*, 2004, **104**, 2833; (*b*) J. Kido and Y. Okamoto, *Chem. Rev.*, 2002, **102**,2357; (*c*) J. Silver, R. Withnall, *Chem. Rev.*, 2004, **104**, 2833.

5 (*a*) Q. M. Wang and B. Yan, *J. Mater. Chem.*, 2004, **14**, 2450; (*b*) J. L. Liu and B. Yan, *J. Phys. Chem. B*, 2008, **112**, 10898; (*c*) B. Yan and H. F. Lu, *Inorg. Chem.*, 2008, **47**, 5601; (*d*) L. Guo, B. Yan and J. L. Liu, *Dalton Trans.*, 2011, **40**, 4933;

6 (*a*) J. Feng, S. Y. Song, W. Q. Fan, L. N. Sun, X. M. Guo, C. Y. Peng, J. B. Y. N. Yu and H. J. Zhang, *Microp. Mesop. Mater.*, 2009, **117**, 278; (*b*) Q. G. Meng, P. Boutinaud, A. C. Franville, H. J. Zhang and R. Mahiou, *Microp. Mesop. Mater.*, 2003, **65**, 127.

7 (*a*) Y. Li, B. Yan and Y. J. Li, *Microp. Mesop. Mater.*, 2010, **132**, 87; (*b*) Y. J. Li, L. Wang and B. Yan, *J. Mater. Chem*., 2011, **21**, 1130.

8 (*a*) L. N. Sun, S. Dang, J. B. Yu, J. Feng, L. Y. Shi and H. J. Zhang *J. Phys. Chem. B*, 2010, **114**, 16393; (*b*) B. Yan and Y. Li, *Dalton Trans.*, 2010, **39**, 1480; (*c*) Y. J. Li, B. Yan and Y. Li, *Chem. Asi. J.*, 2010, **5**, 59.

9 (*a*) D. Zhao, Q. Huo, J. Feng, B. F. Chmelka and G. D. Stucky, *J. Am. Chem. Soc.*, 1998, **120**, 6024; (*b*) Q. P. Li and B. Yan, *Dalton Trans.* 2012, 41, 8567; (*c*) Y. J. Gu and B. Yan, *Eur. J. Inorg. Chem.*, 2013, 296.

10 L. Chen and B. Yan, *Dalton Trans.*, 2014, **43**, 14123.

11 (*a*)M. Kurmoo, *Chem. Soc. Rev.*, 2009, **38**, 1353; (*b*) O. Shekhah, J. Liu, R. A. Fischer and C. Woll,*Chem. Soc. Rev.*, 2011, **40**, 1081; (*c*) A. Betard and R. A. Fischer, *Chem. Rev.*, 2012, **112**, 1055.

12 (*a*) M. D. Allendorf, C. A. Bauer, R. K. Bhakta and R. J. T. Houk,*Chem. Soc. Rev.*, 2009, **38**, 1330; (*b*) J. Rocha, L. D. Carlos, F. A. Almeida Paz and D. Ananias,*Chem. Soc. Rev.*, 2011, **40**, 926; (*c*) Y. J. Cui, Y. F. Yue, G. D. Qian and B. L. Chen,*Chem. Rev.*, 2012, **112**, 1126.

13 (*a*) D. Rocca, D. Liu and W. B. Lin, *Acc. Chem. Res.*, 2011, **44**, 957; (*b*) L. E. Kreno, K. Leong, O. K. Farha, M. Allendorf, R. P. Van Duyne and J. T. Hupp, *Chem. Rev.*, 2012, **112**, 1105; (*d*) P. Horcajada, R. Gref, T. Baati, P. K. Allan, G. Maurin, P. Couvreur, G. Ferey, R. E. Morris and C. Serre, *Chem. Rev.*, 2012, **112**, 1232.

14 (*a*) X. Wang, K. S. K. Lin, J. C. C. Chan and S. Cheng, *J. Phys. Chem. B*, 2005, **109**, 1763; (*b*) L. N. Sun, J. B. Yu, H. J. Zhang, Q. G. Meng, E. Ma, C. Y. Peng and K. Y. Yang, *Microp. Mesop. Mater*., 2007, **98**, 156.

15 (*a*) L. G. DeShazer and G. H. Dieke, *J. Chem. Phys.*, 1963, **38**, 2190; (*b*) W. T. Carnall, P. R. Fields and K. Rajnak, *J. Chem. Phys.*, 1968, **49**, 4450; (*c*) M. D. Regulacio, M. H. Pablico, J. A. Vasquez, P. N. Myers, S. Gentry, M. Prushan, S. W. Tam-Changand and S. L. Stoll, *Inorg. Chem.*, 2008, **47**, 1512.

16 (*a*) H. S. He, A. G. Sykes, D. Galipeau, S. Weng Ng and M. Ropp, *Inorg. Chem. Commun.*, 2008, **11**, 1051; (*b*) J. Feng, J. B. Yu, S. Y. Song, L. N. Sun, W. Q. Fan, X. M. Guo, S. Dang and H. J. Zhang, *Dalton Trans.*, 2009, 2406.

17 (*a*) S. I. Klink, H. Keizer and F. C. J. M. van Veggel, *Angew. Chem. Int. Ed.*, 2000,**39**, 4319; (*b*) I. Oueslati, R. A. S. Ferreira, L. D. Carlos, C. Baleizao, M. N. Berberan-Santos, B. de Castro, J. Vicens and U. Pischel, *Inorg. Chem.*, 2006,**45**, 2652.

